

Supporting Information

A Computational Evaluation of the Mechanism of Penicillin-Binding Protein Catalyzed Cross-linking of the Bacterial Cell Wall

Qicun Shi, Samy O. Meroueh, Jed F. Fisher, and Shahriar Mobashery*

Contribution from the Department of Chemistry and Biochemistry,

University of Notre Dame, Notre Dame, IN 46556

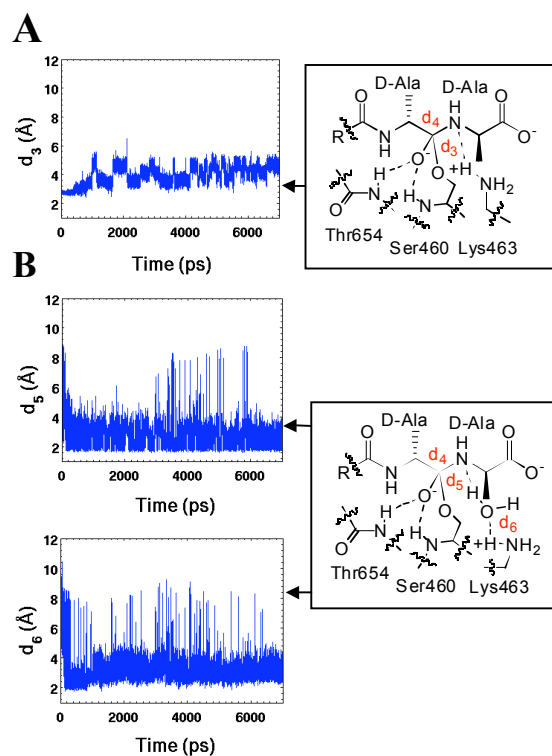


Figure S1. Distances collected from MD sampling simulation, over 7.8 ns, evaluating (A) direct proton transfer (d_3) from Lys463 and (B) water-mediated proton transfer route with dual transfers (d_5 and d_6). Distances (Å) are the separation between amide N and carbonyl C for d_4 ; between the amide N and water H for d_5 ; and between the water O and one of the hydrogens of Lys463 for d_6 .

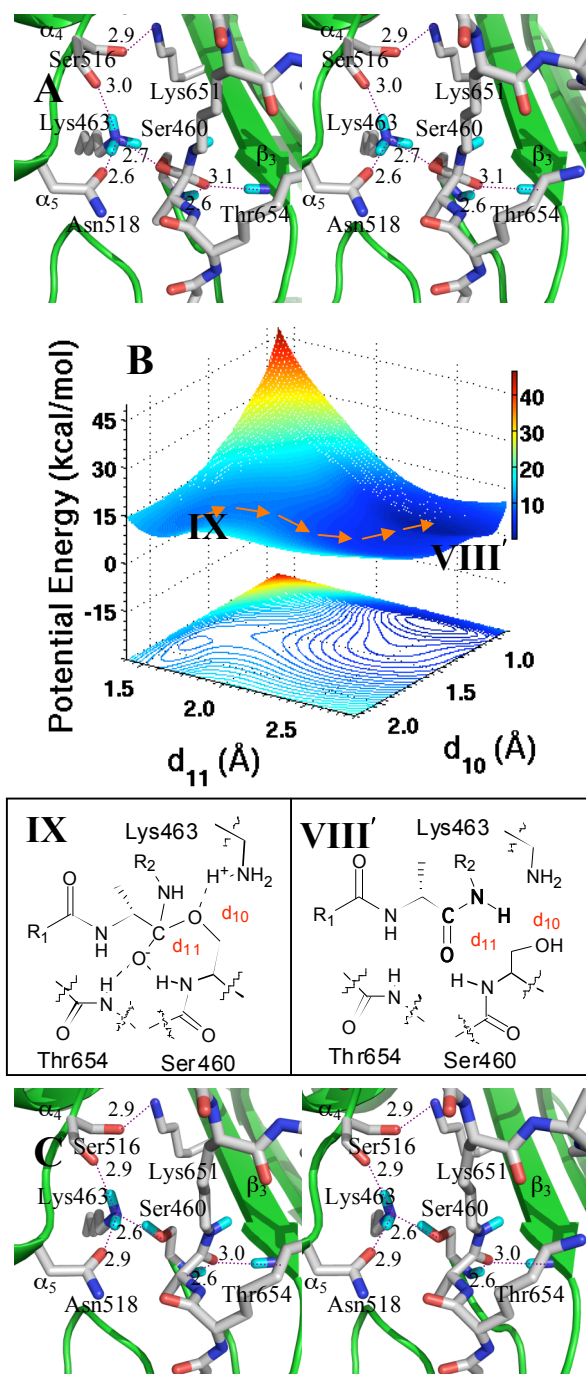


Figure S2. (A) The tetrahedral species (IX) resulting from L-Lys H proton transfer to Lys463. Hydrogen bonds are shown as dashed lines (distances in Å between heteroatoms). The tetrahedral species is nestled between β_3 sheet and the loop connecting the α_4 and α_5 helices. Important active site residues and the tetrahedral species are in capped-stick (C, gray; N, blue; O, red; H, cyan). Distances (Å) are rounded to the nearest tenth. (B) QM/MM potential energy surface and the contour over reaction coordinates represented as a shadow. The reaction path from the tetrahedral species (IX) to the enzyme-product (VIII') is shown with orange arrows. (C) The conformation of the product (VIII') resulting from proton transfer from protonated Lys463 to the ester oxygen with collapse of the tetrahedral.

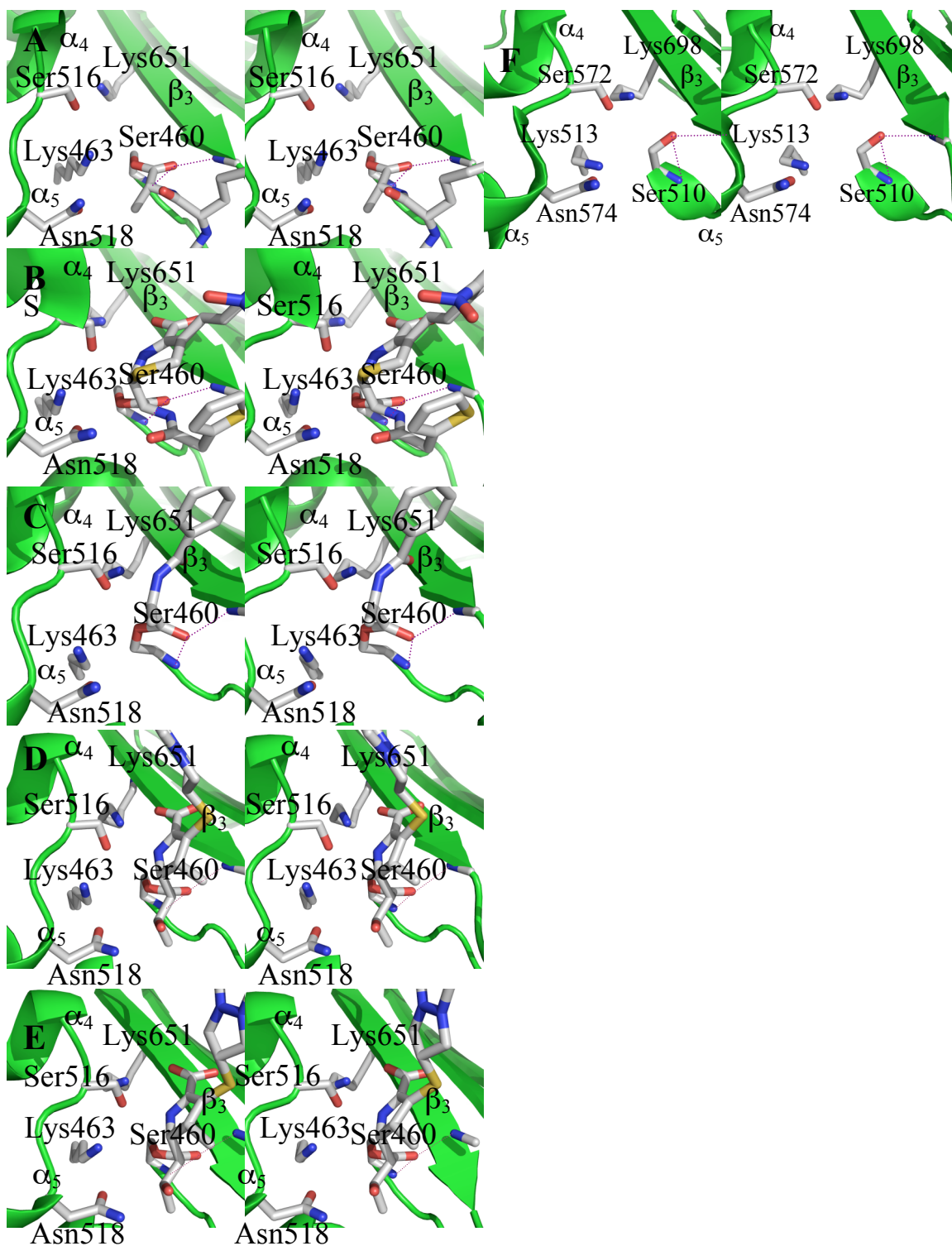


Figure S3. Comparison of the PBP 1b acyl-enzyme from the ONIOM QM/MM calculations (A) and the x-ray structures of PBP 1b complexed with nitrocefim (B); *N*-Benzoyl-D-alanylmercaptoacetic acid thioester (C); PBP 1a complexed with biapenem (D); PBP 2x complexed with biapenem (E); and PBP 6 of *E. coli* (F). The acyl-enzyme intermediates are nestled between β_3 sheet and the loop connecting α_4 and α_5 helices. Important active site residues and the tetrahedral portion are represented in capped-sticks. Two hydrogen bonds (magenta) in the oxyanion hole are shown as dashed lines.

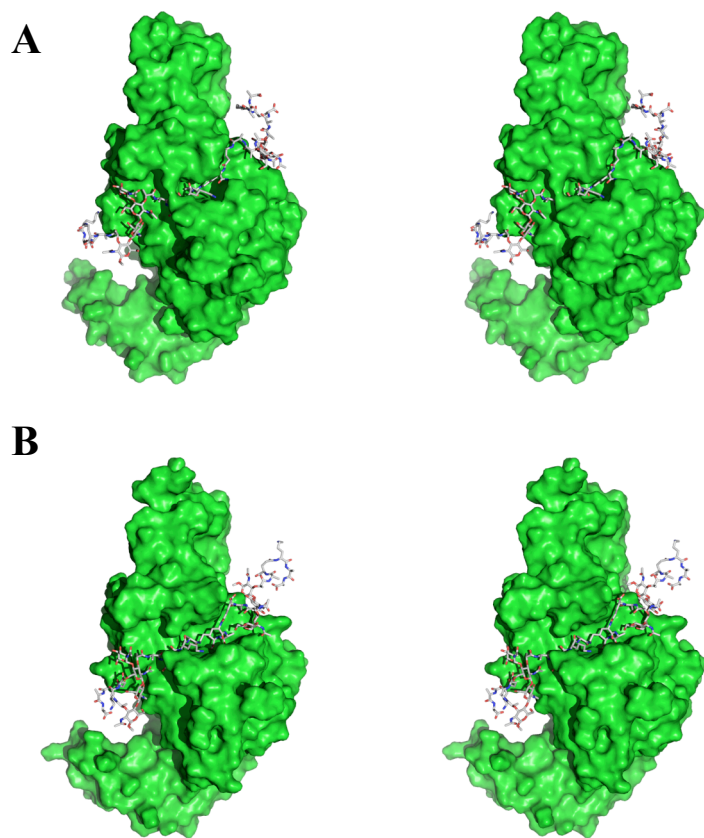


Figure S4. Two snapshots, taken from a 10 ns molecular dynamics simulation of the acyl-enzyme-peptidoglycan acceptor complex, illustrating the closed cleft (A) and the open cleft (B) states.

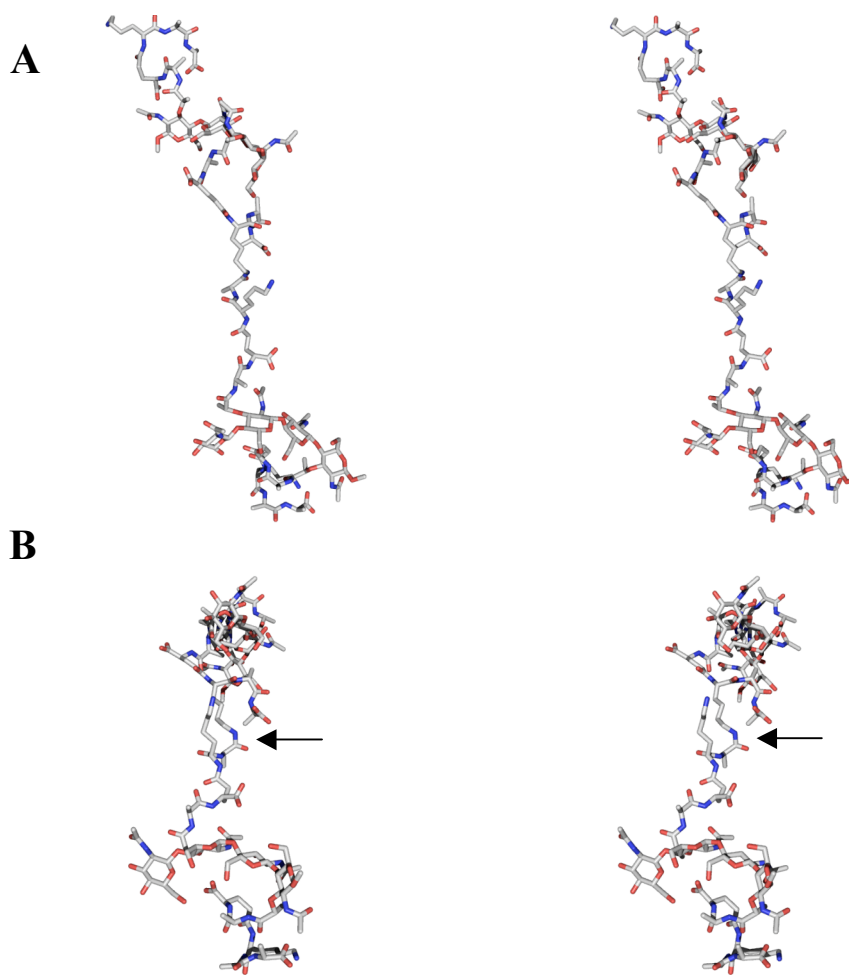


Figure S5. Panel A shows the cross-linked peptidoglycan structure as excised from (and showing the same orientation as is depicted in) **Figure 1E**. In the perspective of Panel A the atoms of the *cis*-amide \rightarrow -D-Ala-L-Lys crosslink are approximately in the orthogonal plane of the paper. Rotation of Panel A by 90° gives Panel B. The *cis*-amide is seen clearly (arrow).

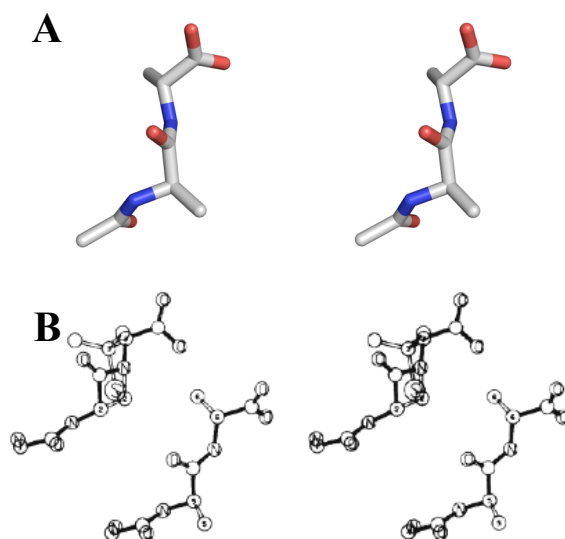


Figure S6. (A) Stereostructure of the conformation of the *N*-acyl-D-Ala-D-Ala stem terminus in the PBP 1b-substrate Michaelis complex. (B) Stereostructures of a tetrahedral-like *N*-acyl-D-Ala-D-Ala conformation (lower right structure of Panel B) spatially matched to a penicillin (upper left structure of Panel B). Panel B is taken from Lee, B. *J. Mol Biol.* **1971**, *61*, 463–469. The spatial concurrence of the -D-Ala-D-Ala conformation in Panel A compared to the lower right conformation in Panel B is very close.